

(In)GaAsN-based type-II “W” quantum-well lasers for emission at $\lambda = 1.55 \mu\text{m}$

I. Vurgaftman^{a)} and J. R. Meyer
Naval Research Laboratory, Code 5613, Washington, DC 20375

N. Tansu and L. J. Mawst
Center for Optical Technologies, Department of Electrical and Computer Engineering, Lehigh University, Bethlehem, PA 18015.

(Received 12 May 2003; accepted 6 August 2003)

Whereas laser emission at $1.55 \mu\text{m}$ is difficult to realize using type-I InGaAsN quantum wells grown on GaAs, we show that it can be achieved with far fewer restrictions on the growth by employing type-II (In)GaAsN/GaAsSb/(In)GaAsN/GaAs structures having a “W” band alignment. We use a 10-band $\mathbf{k}\cdot\mathbf{p}$ formalism that accounts for the N band anticrossing to calculate the gain and spontaneous-emission characteristics of “W” structures optimized for maximum overlap of the electron and hole wave functions. We estimate that one to three wells would be necessary for edge emitters with moderate cavity losses and nonradiative recombination rates, and a somewhat larger number of wells may be required for vertical-cavity surface emitters. © 2003 American Institute of Physics. [DOI: 10.1063/1.1616193]

The current $1.55 \mu\text{m}$ diode laser technology relies almost exclusively on epitaxial growth on InP substrates. Vertical-cavity surface-emitting lasers (VCSELs) are especially challenging, owing to the small refractive-index contrast that is typically available, and InP-based processing is generally less convenient than GaAs based. Although several alternative approaches^{1,2} are under investigation, the ideal solution is to develop an active region that is compatible with growth on GaAs. While GaAs-based lasers with InGaAsN active quantum wells have recently made inroads into the $1.3\text{-}\mu\text{m}$ -edge-emitting³ and VCSEL technology,⁴ reports of emission at longer wavelengths are rather limited.^{5,6} This is due primarily to the difficulty of incorporating In and N alloy fractions that are simultaneously large enough to produce the required energy gap of $\approx 0.8 \text{ eV}$ with high optical quality.

Recently, it has been suggested that instead of employing type-I InGaAsN quantum wells (QWs), longer wavelengths may be accessed more readily via type-II GaAsN/GaAsSb^{7,8} and InGaAsN/GaAsSb (Ref. 8) structures. The energy gap in a type-II structure is governed primarily by the relative conduction and valence band alignments in two adjacent layers rather than by the bulk gap in a single layer. The resulting flexibility comes at the expense of reduced overlap between the electron and hole wave functions that now peak in different layers. In the midwave-infrared ($3\text{--}5 \mu\text{m}$) spectral range, an approach that has found wide acceptance is the so-called “W” structure,^{9,10} in which two electron QWs sandwich a single hole QW to maximize the type-II wave function overlap and hence the differential gain. InGaAs/GaAsPSb “W” structures for emission at 1.3 and $1.55 \mu\text{m}$ have also been studied.¹¹ In this letter, we propose an optimized dilute-nitride type-II “W” design for emission at $\lambda = 1.55 \mu\text{m}$, and analyze in detail its gain and spontaneous

emission characteristics. Implications for the design of GaAs-based edge emitters and VCSELs are discussed.

The band diagram for one period of an optimized structure with $\approx 0.8\text{-eV}$ -energy gap at room temperature is shown in Fig. 1. Each of the two GaAs_{0.97}N_{0.03} electron QWs is 15 \AA thick, as is the single GaAs_{0.65}Sb_{0.35} hole QW. The GaAsN QWs are in turn surrounded by GaAs barriers (50 \AA thick), although the simulated device properties are marginally improved if GaAsP barriers are used instead. While the single-period unit illustrated in Fig. 1 is not strain compensated, the layers are thin enough and the anticipated number of periods small enough that the imbalance may be acceptable. One alternative is to compensate the net compressive strain of the QW layers by employing GaAsP barriers with adjusted P

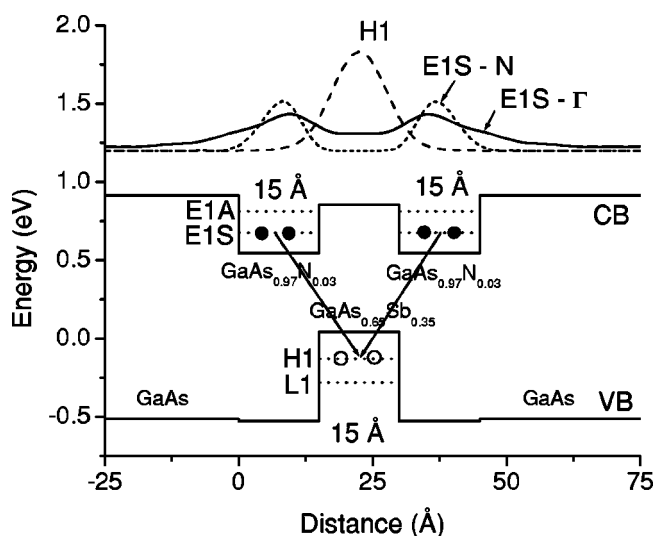


FIG. 1. Band diagram and selected wave function components for one period of the 15 \AA GaAs_{0.97}N_{0.03}/ 15 \AA GaAs_{0.65}Sb_{0.35}/ 15 \AA GaAs_{0.97}N_{0.03}/ 50 \AA GaAs W active region optimized for emission at $1.55 \mu\text{m}$.

^{a)}Electronic mail: vurgaftman@nrl.navy.mil

content. Since adequate hole confinement often becomes an issue when type-I GaAsN and InGaAsN active regions are employed, the strong confinement of both carrier types (even if a GaAsP barrier is not used) here represents an additional advantage of the type-II approach.⁹

Energy dispersion relations, wave functions, and optical matrix elements were calculated using a 10-band (N-like, Γ -like conduction, heavy-, light-, and split-off hole) $\mathbf{k}\cdot\mathbf{p}$ formalism. The band anticrossing (BAC) model¹² is employed to incorporate a spin-degenerate nitrogen-like band^{13,14} that accounts for the interaction of Γ - and N-like states in the dilute-nitride layers. A similar approach was recently used to calculate the characteristics of type-I InGaAsN QW structures for emission at 1.3 μm .¹⁵ Band parameters for the non-nitride and dilute-nitride materials are taken from our recent reviews.^{16,17} Briefly, for GaAsN, we employ a coupling potential of $V=2.7$ eV, along with an N level that is 0.228 eV higher than the GaAs conduction band minimum at 300 K. It is assumed that the interaction with the N level does not affect the position of the valence band in the dilute-N material. The unstrained valence-band offset (VBO) of GaAs_{0.65}Sb_{0.35} with respect to GaAs is taken to be 0.51 eV.^{16,18,19} While that parameter remains somewhat controversial (see in particular the cited works and the corresponding discussion in Ref. 16) the uncertainty affects only the details and not the main qualitative trends of our simulation study. The inclusion of compressive strain in GaAsSb increases the GaAs/GaAsSb VBO to 0.593 eV for the heavy-hole band, and a weakly type-II alignment at the GaAs/GaAsSb hetero-interface results in a conduction-band offset of 0.16 eV at 300 K. The GaAs/GaAsN unstrained VBO is most likely quite small, and for definiteness is assumed to vanish.¹⁷ In the dilute-N layer, the effect of strain is included into the position of the conduction band of the host (nitrogen-free) material, and the interaction with the N level is then introduced as for the unstrained material. The resulting Hamiltonian is diagonalized in reciprocal space, with a wave vector cutoff of $\approx 0.2(2\pi/a)$ in order to avoid the introduction of spurious states.

Figure 1 also shows selected results for the electron and hole subband energies and wave functions. The 136 meV splitting between the symmetric (E1S) and antisymmetric (E1A) electron subbands⁹ is sufficient to limit the thermal population of nonlasing E1A states at room temperature under typical injection conditions. The heavy/light hole splitting of 151 meV should similarly assure that most of the holes occupy H1 lasing states, while being small enough to provide a potential mechanism for interperiod transport via light-hole tunneling at room temperature. The E1S miniband width of 10 meV, which may be adjusted by varying either the thickness or the composition of the GaAs(P) barriers, is sufficient to permit interperiod electron tunneling without having a significant impact on the differential gain at 300 K. The H1 dispersion along the growth direction is negligible.

Owing to the strong coupling between Γ - and N-like states in the GaAsN layer, the E1S wave function has two significant components. According to our calculations, $\approx 35\%$ of that wave function is N-like at the zone center and does not contribute to the optical gain. It can be seen from the wave functions in Fig. 1 that the N-like component is

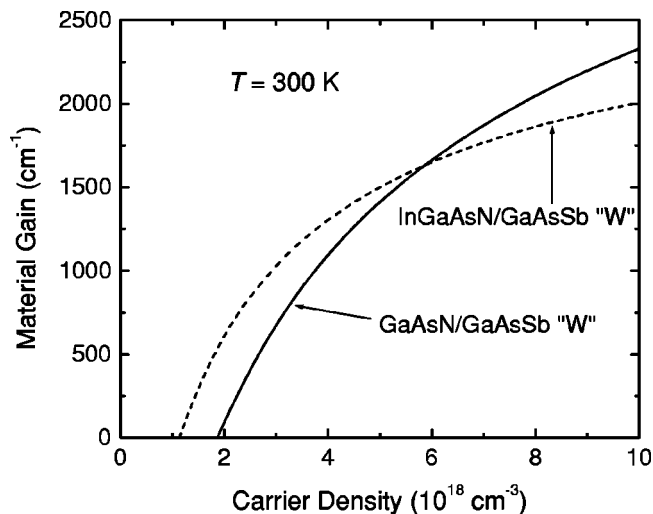


FIG. 2. Material gain as a function of injected carrier density at 300 K for the structure of Fig. 1 (solid), and for the 25 \AA In_{0.3}Ga_{0.7}As_{0.975}N_{0.025}/15 \AA GaAs_{0.65}Sb_{0.35}/25 \AA In_{0.3}Ga_{0.7}As_{0.975}N_{0.025}/50 \AA GaAs W structure (dashed).

strongly localized in the GaAsN layers, whereas the Γ -like component exhibits appreciable overlap with H1. We estimate that the square of the optical matrix element at the zone center in the W structure of Fig. 1 is $\approx 25\%$ of that in bulk GaAs. This ratio is comparable to that computed for antimonide W structures.⁹ We emphasize that the W configuration should be much more attractive than a simple two-constituent GaAsN/GaAsSb superlattice with strong electron dispersion along the growth axis, owing to the higher density of states near the band edge and also the appreciable optical matrix element throughout the electron miniband.

Using the computed subband dispersions and wave functions, and a Gaussian broadening linewidth of 5 meV, we have calculated optical gain and spontaneous-emission characteristics. The calculations incorporate the impact of band filling at the corresponding carrier densities, although the effects of heating, which are expected to be modest near the lasing threshold are not included. We focus on two representative W structures: (1) that of Fig. 1 and (2) a 25 \AA In_{0.3}Ga_{0.7}As_{0.975}N_{0.025}/15 \AA GaAs_{0.65}Sb_{0.35}/25 \AA In_{0.3}Ga_{0.7}As_{0.975}N_{0.025}/50 \AA GaAs active region, which has the same energy gap but slightly larger matrix element at the zone center. While the latter structure requires quaternary dilute-nitride layers, it is more forgiving from the standpoint of thicker electron QWs. Both structures should be practical to grow by either molecular beam epitaxy (MBE) or metal-organic chemical vapor deposition (MOCVD).

Calculated material gains as a function of carrier density are shown in Fig. 2 for the two structures at room temperature. The transparency carrier densities are 1.8 and 1.2 $\times 10^{18} \text{ cm}^{-3}$, and the differential gains near transparency are 6.5 and 8.0 $\times 10^{-16} \text{ cm}^2$ for the structures with GaAsN and InGaAsN, respectively. The differential-gain values may be compared with 1.5–2.0 $\times 10^{-15} \text{ cm}^2$ for strained InGaAs QWs on GaAs emitting near $\lambda=1 \mu\text{m}$ and 1.0–1.5 $\times 10^{-15} \text{ cm}^2$ for strained InGaAs wells on InP emitting near $\lambda=1.5 \mu\text{m}$.^{20,21} A lower bound on the threshold current density may be obtained by calculating the radiative recombination rate. Resulting material gains as a function of radiative current density are shown in Fig. 3 for single periods of the

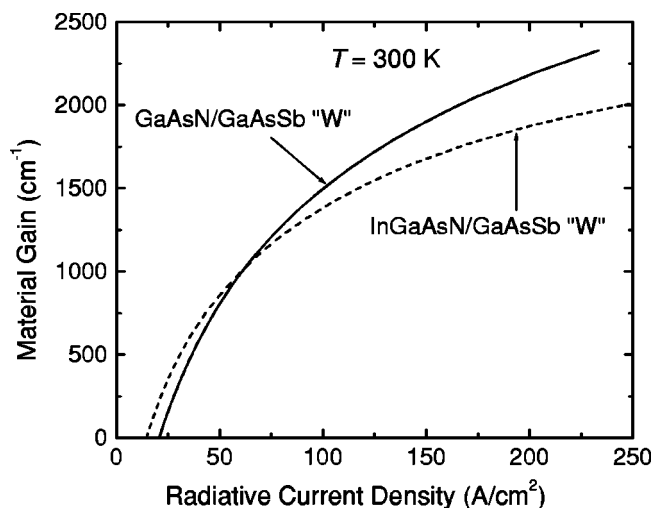


FIG. 3. Material gain as a function of radiative current density at 300 K for same two structures.

two W structures. We find that the InGaAsN structure displays only a modest advantage over the GaAsN structure in terms of radiative current density near transparency, and the maximum gain under strong injection is actually lower. The InGaAsN structure may be advantageous if relatively low optical gain is required and Auger recombination dominates, since its threshold carrier density may be much lower (Fig. 2). Because the GaAsSb hole QW is thin and compressively strained, the W structure of Fig. 1 has good prospects for suppressing the CCCH Auger process.

It is apparent from Figs. 2 and 3 that as long as no more than $\approx 1500 \text{ cm}^{-1}$ of gain is required, radiative recombination dominates, and the linewidth is not significantly broader than 5 meV, a single stage of either W structure should be adequate. The surprisingly high maximum gain (despite the lower type-II matrix element) may be attributed in part to the electron mass enhancement (m_e is heavier than in bulk GaAs) associated with the interaction between the Γ and N bands. This increases the density of states, and also brings the electron/hole mass ratio much closer to unity (≈ 0.5 , as compared to 0.2 in bulk GaAs). The comparable electron and hole masses should also reduce the linewidth enhancement factor in these lasers.

We finally examine the implications of the gain curves in Figs. 2 and 3 for the design of edge and surface emitting lasers with dilute-nitride W active QWs. We assume that the waveguide for the edge emitter includes 1.1- μm -thick $\text{Al}_{0.74}\text{Ga}_{0.26}\text{As}$ n and p claddings and 0.2- μm -thick GaAs separate-confinement regions on both sides of the active QWs.²² This waveguide yields an optimized optical confinement factor of 2.2%/well. A single stage may then be sufficient as long as the total loss (internal+mirror) does not exceed $\approx 30 \text{ cm}^{-1}$. However, if the broadening and/or non-radiative recombination are less favorable than those assumed here, or if short devices are desired for high-speed operation, two or three periods of the W structure may be required.

The mirror loss per pass for a GaAs-based VCSEL may be $< 0.5\%$,²³ although somewhat higher values are often found in working devices. Provided the active QWs are placed at a maximum of the optical field (which enhances the modal gain by up to a factor of 2), three or more wells may need to be employed. Although the uniformity of hole injection becomes an important issue as the number of wells is increased, no significant nonuniformity is apparent in mid-infrared antimonide W lasers with a similar valence-band alignment and heavy-light hole splitting.²⁴

The envisioned GaAs-based edge-emitting diodes and VCSELs with dilute-nitride W active regions may be expected to display significant practical advantages over InP-based lasers emitting at $\lambda = 1.55 \mu\text{m}$. Our calculated results for the gain and spontaneous-emission characteristics demonstrate that these type-II structures offer a promising foundation for GaAs-based telecommunications sources.

- ¹J. Boucart, C. Starck, F. Gaborit, A. Plais, N. Bouche, E. Derouin, J. C. Remy, J. Bonnet-Gamard, L. Goldstein, C. Fortin, D. Carpentier, P. Salet, F. Brillouet, and J. Jacquet, *IEEE J. Sel. Top. Quantum Electron.* **5**, 520 (1999).
- ²Y. Ohiso, H. Okamoto, R. Iga, K. Kishi, and C. Amano, *IEEE Photonics Technol. Lett.* **14**, 738 (2002).
- ³N. Tansu and L. J. Mawst, *IEEE Photonics Technol. Lett.* **14**, 444 (2002).
- ⁴K. D. Choquette, J. F. Klem, A. J. Fischer, O. Blum, A. A. Allerman, I. J. Fritz, S. R. Kurtz, W. G. Breiland, R. Sieg, K. M. Geib, J. W. Scott, and R. L. Naone, *Electron. Lett.* **36**, 1388 (2000).
- ⁵M. O. Fischer, M. Reinhardt, and A. Forchel, *IEEE J. Sel. Top. Quantum Electron.* **7**, 149 (2001).
- ⁶W. Ha, V. Gambin, M. Wistey, S. Bank, S. Kim, and J. S. Harris, Jr., *IEEE Photonics Technol. Lett.* **14**, 591 (2003).
- ⁷P. D. Dapkus, International Patent Application No. PCT/US00/14332 (WO01/29943), May 24, 2000.
- ⁸N. Tansu and L. J. Mawst, *IEEE J. Quantum Electron.* (in press).
- ⁹J. R. Meyer, C. A. Hoffman, F. J. Bartoli, and L. R. Ram-Mohan, *Appl. Phys. Lett.* **67**, 757 (1995).
- ¹⁰I. Vurgaftman, C. L. Felix, W. W. Bewley, D. W. Stokes, R. E. Bartolo, and J. R. Meyer, *Philos. Trans. R. Soc. London, Ser. A* **359**, 489 (2001).
- ¹¹P. Dowd, W. Braun, D. J. Smith, C. M. Ryu, C.-Z. Guo, S. L. Chen, U. Koelle, S. R. Johnson, and Y.-H. Zhang, *Appl. Phys. Lett.* **75**, 1267 (1999).
- ¹²J. Wu, W. Shan, and W. Walukiewicz, *Semicond. Sci. Technol.* **17**, 860 (2002).
- ¹³S. A. Choulis, T. J. C. Hosea, S. Tomic, M. Kamal-Saadi, A. R. Adams, E. P. O'Reilly, B. A. Weinstein, and P. J. Klar, *Phys. Rev. B* **66**, 165321 (2002).
- ¹⁴S. A. Choulis, S. Tomic, E. P. O'Reilly, and T. J. C. Hosea, *Solid State Commun.* **125**, 155 (2003).
- ¹⁵S. Tomic and E. P. O'Reilly, *IEEE Photonics Technol. Lett.* **15**, 6 (2003).
- ¹⁶I. Vurgaftman, J. R. Meyer, and L. R. Ram-Mohan, *J. Appl. Phys.* **89**, 5815 (2001).
- ¹⁷I. Vurgaftman and J. R. Meyer, *J. Appl. Phys.* **94**, 3675 (2003).
- ¹⁸J. Hu, X. G. Xu, J. A. H. Stotz, S. P. Watkins, A. E. Curzon, M. L. W. Thewalt, N. Matine, and C. R. Bolognesi, *Appl. Phys. Lett.* **73**, 2799 (1998).
- ¹⁹P. W. Yu, D. C. Reynolds, B. Jogai, J. Loehr, and C. E. Stutz, *Appl. Phys. Lett.* **61**, 2317 (1992).
- ²⁰S. W. Corzine, R. H. Yan, and L. A. Coldren, *Appl. Phys. Lett.* **57**, 2835 (1990).
- ²¹S. W. Corzine and L. A. Coldren, *Appl. Phys. Lett.* **59**, 588 (1991).
- ²²N. Tansu, N. J. Kirsch, and L. J. Mawst, *Appl. Phys. Lett.* **81**, 2523 (2002).
- ²³R. S. Geels, B. J. Thibeault, S. W. Corzine, J. W. Scott, and L. A. Coldren, *IEEE J. Quantum Electron.* **29**, 2977 (1993).
- ²⁴W. W. Bewley, H. Lee, I. Vurgaftman, R. J. Menna, C. L. Felix, R. U. Martinelli, D. W. Stokes, D. Z. Garbuzov, J. R. Meyer, M. Maiorov, J. C. Connolly, A. R. Sugg, and G. H. Olsen, *Appl. Phys. Lett.* **76**, 256 (2000).